Advanced Process Control of the Critical Dimension in Photolithography

Chien-Feng Wu [1], Chih-Ming Hung [1], Juhn-Horng Chen [2] and An-Chen Lee [1,#]

1Department of Mechanical Engineering, National Chiao Tung University, Hsinchu, 300, Taiwan, R.O.C.
2 Department of Mechanical Engineering, Chung Hua University, Hsinchu, 300, Taiwan, R.O.C.
Corresponding Author / E-mail: aclee@mail.nctu.edu.tw; TEL: +886-3-5728513; FAX: +886-3-5725372

KEYWORDS: Run-to-run (R2R) controller, Nonlinear multiple exponential-weight moving-average controller, Dynamic model-tuning minimum-variance (DMTMV) controller, Photolithography process

This paper describes two run-to-run controllers, a nonlinear multiple exponential-weight moving-average (NMEWMA) controller and a dynamic model-tuning minimum-variance (DMTMV) controller, for photolithography processes. The relationships between the input recipes (exposure dose and focus) and output variables (critical dimensions) were formed using an experimental design method, and the photolithography process model was built using a multiple regression analysis. Both the NMEWMA and DMTMV controllers could update the process model and obtain the optimal recipes for the next run. Quantified improvements were obtained from simulations and real photolithography processes.

Manuscript received: September 10, 2007 / Accepted: December 7, 2007

1. Introduction

In semiconductor manufacturing, having more integrated circuit (IC) devices on a large wafer is important from a cost-reduction perspective. Integrated circuit patterns are created on wafers by photolithography, in which optical methods are used to transfer the circuit patterns from master images called masks (1:1) or reticles (4:1) to a thin film of light-sensitive material (photoresist), and are then distributed evenly on the wafer surface. The pattern obtained defines the IC regions protected against the etching process, which will only act on the zones uncovered by the resist mask. After etching, the resist film is removed and the photolithography process is repeated to make the next layer. Photolithography is the primary method used for pattern definitions in nearly all ICs fabricated today, and consists of six steps: resist coating, prebaking, exposing, postexposure baking, developing, and metrology. As the pattern features decrease, controlling the stability of the process becomes more difficult. The pattern outputs of concern to lithographers are the line width (*e.g.*, critical dimension) and overlay.

The critical dimension (CD) is defined as the width of a photoresist line (or space) printed on a test pattern specifically designed to characterize the performance of the lithographic process. As the critical dimension becomes smaller, the line width control becomes more difficult. Crisalle *et al.*[1] designed an adaptive feedback control for the line width. The control structure of their work consisted of a reduced-order lithography model, a parameter estimator, and a nonlinear model-inversion controller. The CD was controlled by adjusting the exposure dose. The control performance was tested using the PROLITH simulator, which demonstrated that the controller was capable of tracking step changes in the CD target, rejecting step disturbances in the resist thickness, resist absorptivity, and focusing. However, it is not practical to implement such a controller online because the film thickness is not often measured for product wafers, and the relationship between the CD and dose is too complex. Lachman-Shalem *et al.*[2] formulated an approach for CD control that combines genetic programming (GP) and nonlinear model predictive (NMP) control. The GP algorithm identified the inputs with the most impact on the CD and generated the best multivariable empirical model for developing the NMP controller. The simulation results obtained from a PROLITH test showed the superiority of their multivariate NMP control on a conventional feedback controller when accounting for manipulated variable constraints. However, such performance of their controller can only be achieved if automation and *in situ* CD measurements are available. Grosman *et al.*[3] published another paper based on the same method. They used a simulated photolithography track and applied the KLA-Tencor-FINLE PROLITHO package calibrated for matching FAB conditions to tune and test the NMPC regulator. However, no real tests were reported and this tuning was executed without any simulated noise. Chemali *et al.*[4] developed three run-to-run feedback controllers using a Kalman filter. Similar to Lachman-Shalem *et al.*[2], they used PROLITH to build the predictive process models and postulated a linear constant process relating the outputs to the inputs. The quantified results revealed the advantage of using the focus as a proper control input for controlling the resist profile. Nevertheless, too many assumptions were made under ideal conditions in their theory, making realization difficult in practice. Yang *et al.*[5] proposed a new statistical formula for monitoring the average CD difference in indistinguishable multi-process patterns and used it to obtain a compensative method.

The lateral positioning between layers comprising ICs is the overlay, which is formally defined as a vector quantity that is the difference between the vector position of a substrate geometry and the vector position of the corresponding point in an overlaying pattern at every point on the wafer.[6] Park *et al.*[7] presented a new run-to-run control scheme to reduce overlay misalignment errors in steppers and

demonstrated the feasibility of their scheme with real-time experimental tests. Their control scheme was designed to find the stepper inputs while minimizing the misalignment errors based on historic data analyses and neural network models. Lee *et al.*[8] measured the overlay error on a real process pattern using a scanning electron microscope (SEM) to overcome the resolution limitations of optical tools. The measured overlay was confirmed using an e-beam inspection tool.

This paper focuses on CD control in photolithography. The experimental design and a multiple regression analysis are used to form relationships between the factors (dose and focus) and the quality property (critical dimension). Then, two controllers, a nonlinear multiple exponential-weight moving-average (NMEWMA) controller and a dynamic model-tuning minimum-variance (DMTMV) controller, are proposed for photolithography processes. Both simulation results and experimental verifications are presented to show the effectiveness of the NMEWMA and DMTMV controllers. Both controllers could easily update the dynamic model and obtain the optimal inputs for the next run. The simulation results demonstrated that the DMTMV controller was more powerful than the NEWMA controller for rejecting disturbances and increasing yields.

2. Experimental Design

The main propose of the experimental design is to build the relationships between the factors (dose and focus) and the quality property (critical dimension), and use the model to realize the run-to-run control. The experiment was a 7^2 factorial design experiment (two factors, seven levels) that was repeated twice. TEL Mark-8 TRACK was used to coat and develop the wafers, a Canon FPA3000 stepper was used to align and expose the wafers, and a Hitachi critical dimension scanning electron microscope (CDSEM) was used to measure the CD data. Table 1 shows the experiment design and results. The experimental data were analyzed with STATISTICA. The three-dimensional (3-D) focus–dose-CD response surface is plotted in Fig. 1. Using a multiple regression analysis, one can build the photolithography process model as

$$Y = 0.424081 - 0.014895X_1 + 0.163589X_2 + 0.146964X_2^2 + \varepsilon \quad (1)$$

$$R_{adj}^2 = 0.98660826\,,$$

where Y is the process output (CD), X_1 and X_2 are the process input recipes (dose and focus, respectively), ε is the process disturbance $\varepsilon \sim NID(0, 0.00525^2)$, and R_{adj}^2 is used to adjust the R^2 statistical quantity. Assuming the output Y of the t^{th} run is related to the input X on the $t-1^{\text{th}}$ run, the process model can be expressed by a nonlinear time series model as

$$Y_t = 0.424081 - 0.014895X_{t-1,1} + 0.163589X_{t-1,2} + 0.146964X_{t-1,2}^2 + \varepsilon_t \quad (2)$$

Let

$$y_t = [Y_t] \quad \mathbf{u}_t = \begin{bmatrix} X_{t,1} \\ X_{t,2} \end{bmatrix} \quad z_t = \left[X_{t,2}^2\right]$$

$$\mathbf{N} = \begin{bmatrix} -0.014895 \\ 0.163589 \end{bmatrix}^T \qquad M = [0.146964]$$

$$a = 0.424018\,.$$

Equation (1) can be rewritten as

$$y_t = \mathbf{N}\mathbf{u}_{t-1} + Mz_{t-1} + a + \varepsilon_t\,. \quad (3)$$

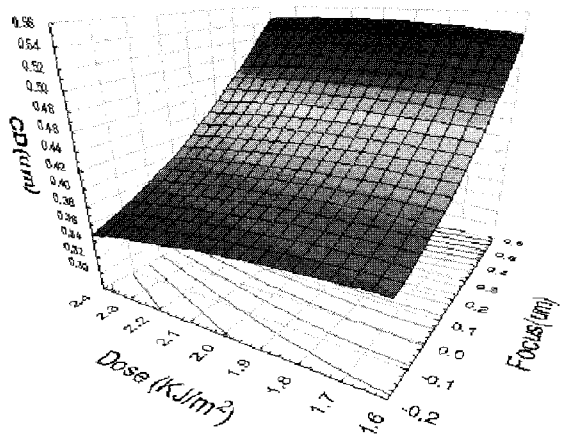

Fig. 1 Focus–dose-CD response surface

3. NMEWMA Controller

Tseng *et al.*[9] proposed a multivariable exponential weight moving average (MEWMA) controller for a linear MIMO process. The linear ($m \times n$) MIMO process ($m \geq n$) assumed by Tseng *et al.*[9] can be described as

$$\mathbf{y}_t = \mathbf{N}\mathbf{u}_{t-1} + \mathbf{a} + \boldsymbol{\varepsilon}_t\,, \quad (4)$$

where $\mathbf{u}_{t-1}$ is a vector of m input recipes and $\mathbf{y}_t$ is a vector of n output variables. The intercept estimate at run $t+1$ is expressed as

$$\hat{\mathbf{a}}_{t+1} = \omega(\mathbf{y}_t - \mathbf{N}\mathbf{u}_{t-1}) + (1-\omega)\hat{\mathbf{a}}_t\,, \quad (5)$$

where ω is a discount factor ($0 < \omega < 1$) and $(\mathbf{y}_t - \mathbf{N}\mathbf{u}_{t-1})$ is the measurement of the intercept at run t. The new recipe $\mathbf{u}_t$ can be obtained by minimizing the following performance index:

$$J = (\mathbf{u}_t - \mathbf{u}_{t-1})^T(\mathbf{u}_t - \mathbf{u}_{t-1}) \quad (6)$$

subjected to

$$\boldsymbol{\tau} = \mathbf{N}\mathbf{u}_t + \hat{\mathbf{a}}_{t+1}\,, \quad (7)$$

where $\boldsymbol{\tau}$ is the target vector. Since $\mathbf{N}^{-1}$ may not exist, multiple $\mathbf{u}_t$ matrices satisfy the constraint. The intuitive meaning of this controller is that one wants to bring the mean of the process output to the desired target with the smallest number of adjustments. By using the method of Lagrange multipliers, the new recipe can be written as

$$\mathbf{u}_t = \left[\mathbf{I} - \mathbf{N}^T\left(\mathbf{N}\mathbf{N}^T\right)^{-1}\mathbf{N}\right]\mathbf{u}_{t-1} + \mathbf{N}^T\left(\mathbf{N}\mathbf{N}^T\right)^{-1}\left(\boldsymbol{\tau} - \hat{\mathbf{a}}_{t+1}\right). \quad (8)$$

For the nonlinear MISO photolithography process described by Eq. (3), the measurement of the intercept at run t can be expressed as $(\mathbf{y}_t - \mathbf{N}\mathbf{u}_{t-1} - Mz_{t-1})$ and the estimate of the intercept at run $t+1$ can be modified to

Table 1 Experimental design

Exp. No.	Dose (KJ/m^2)	Focus (μm)	CD (μm)	Exp. No.	Dose (KJ/m^2)	Focus (μm)	CD (μm)
1	1.7	–0.1	0.3854 0.3824	26	2	0.3	0.4569 0.4585
2	1.7	0	0.4023 0.3969	27	2	0.4	0.4859 0.4852
3	1.7	0.1	0.4189 0.4190	28	2	0.5	0.5195 0.5058
4	1.7	0.2	0.4347 0.4345	29	2.1	–0.1	0.3791 0.3731
5	1.7	0.3	0.4655 0.4578	30	2.1	0	0.3927 0.3951
6	1.7	0.4	0.4856 0.4786	31	2.1	0.1	0.4164 0.4068
7	1.7	0.5	0.5121 0.5039	32	2.1	0.2	0.4302 0.4345
8	1.8	–0.1	0.3896 0.3853	33	2.1	0.3	0.4571 0.4601
9	1.8	0	0.3999 0.3907	34	2.1	0.4	0.4851 0.4884
10	1.8	0.1	0.4199 0.4138	35	2.1	0.5	0.5149 0.5047
11	1.8	0.2	0.4372 0.4347	36	2.2	–0.1	0.3779 0.3720
12	1.8	0.3	0.4604 0.4574	37	2.2	0	0.3948 0.3891
13	1.8	0.4	0.4876 0.4793	38	2.2	0.1	0.4097 0.4109
14	1.8	0.5	0.5181 0.5109	39	2.2	0.2	0.4275 0.4283
15	1.9	–0.1	0.3870 0.3793	40	2.2	0.3	0.4557 0.4590
16	1.9	0	0.4025 0.3939	41	2.2	0.4	0.4783 0.4802
17	1.9	0.1	0.4246 0.4189	42	2.2	0.5	0.5109 0.5080
18	1.9	0.2	0.4329 0.4288	43	2.3	–0.1	0.3772 0.3576
19	1.9	0.3	0.4590 0.4591	44	2.3	0	0.3818 0.3770
20	1.9	0.4	0.4847 0.4836	45	2.3	0.1	0.4021 0.3992
21	1.9	0.5	0.5151 0.5112	46	2.3	0.2	0.4265 0.4202
22	2	–0.1	0.3886 0.3810	47	2.3	0.3	0.4562 0.4539
23	2	0	0.3994 0.3932	48	2.3	0.4	0.4818 0.4756
24	2	0.1	0.4192 0.4091	49	2.3	0.5	0.5234 0.5196
25	2	0.2	0.4301 0.4310				

$$\hat{a}_{t+1} = \omega(y_t - \mathbf{N}\mathbf{u}_{t-1} - Mz_{t-1}) + (1-\omega)\hat{a}_t . \tag{9}$$

Then, a one-step-ahead forecast of output can be obtained from

$$\hat{y}_{t+1} = \mathbf{N}\mathbf{u}_t + Mz_t + \hat{a}_{t+1} . \tag{10}$$

The minimum-variance control algorithm[10–12] is adopted for the nonlinear processes to obtain the new formula. With the minimum-variance control criterion, the performance index in the MISO case is

$$\begin{aligned} J &= (\hat{y}_{t+1} - \tau)W(\hat{y}_{t+1} - \tau) + (\mathbf{u}_t - \mathbf{u}_{t-1})^T \mathbf{\Gamma}(\mathbf{u}_t - \mathbf{u}_{t-1}) \\ &= (\mathbf{N}\mathbf{u}_t + Mz_t + \hat{a}_{t+1} - \tau)W(\mathbf{N}\mathbf{u}_t + Mz_t + \hat{a}_{t+1} - \tau), \\ &\quad + (\mathbf{u}_t - \mathbf{u}_{t-1})^T \mathbf{\Gamma}(\mathbf{u}_t - \mathbf{u}_{t-1}) \end{aligned} \tag{11}$$

where τ is the CD target. Unlike the controller used in the MEWMA method, the process engineer can select the scale W and matrix $\mathbf{\Gamma}$ to weigh the importance of minimizing the variance of the outputs around their targets against minimizing the variance of the inputs. It is not feasible to derive a closed form of the minimum-variance controller for a MISO process as described by Eq. (3) when nonlinear effects of inputs are present. Many optimization techniques,[13] such as genetic algorithms, are available to search for the optimal input to minimize the performance index. For simplicity, one can replace z_t with z_{t-1} in Eq. (11), differentiate it with respect to $\mathbf{u}_t$ and let it equal to zero:

$$\frac{\partial J}{\partial \mathbf{u}_t} = 0 . \tag{12}$$

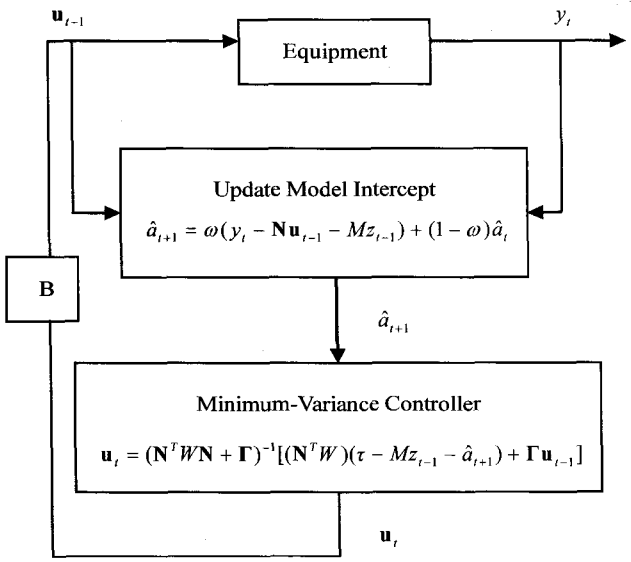

Fig. 2 Block diagram of a NMEWMA controller

Then, a suboptimal formula of the next run can be obtained from

$$\mathbf{u}_t = (\mathbf{N}^T W\mathbf{N} + \mathbf{\Gamma})^{-1}[(\mathbf{N}^T W)(\tau - Mz_{t-1} - \hat{a}_{t+1}) + \mathbf{\Gamma}\mathbf{u}_{t-1}] . \tag{13}$$

A block diagram of the NMEWMA controller is shown in Fig. 2.

4. DMTMV Controller

A NMEWMA controller assumes that the process model is invariant and only the intercept is disturbed. However, the process model may change with time so that it becomes essential to simultaneously forecast the output and tune the model coefficients. Many recursive least-squares algorithms have been proposed.[14–16] If the process model varies with time, a one-step-ahead forecast of the output can be rewritten as

$$\hat{y}_t = \hat{\mathbf{N}}_t\mathbf{u}_{t-1} + \hat{M}_t z_{t-1} + \hat{a}_t . \tag{14}$$

If we define the input vector as

$$\boldsymbol{\varphi}_{t-1}^T = \left[\mathbf{u}_{t-1}^T \mid z_{t-1} \mid 1\right] \tag{15}$$

and the coefficient vector estimate as

$$\hat{\boldsymbol{\theta}}_t^T = \left[\hat{\mathbf{N}}_t^T \mid \hat{M}_t \mid \hat{a}_t\right], \tag{16}$$

then the one-step-ahead forecast of the output is

$$\hat{y}_t = \boldsymbol{\varphi}_{t-1}^T \cdot \hat{\boldsymbol{\theta}}_t . \tag{17}$$

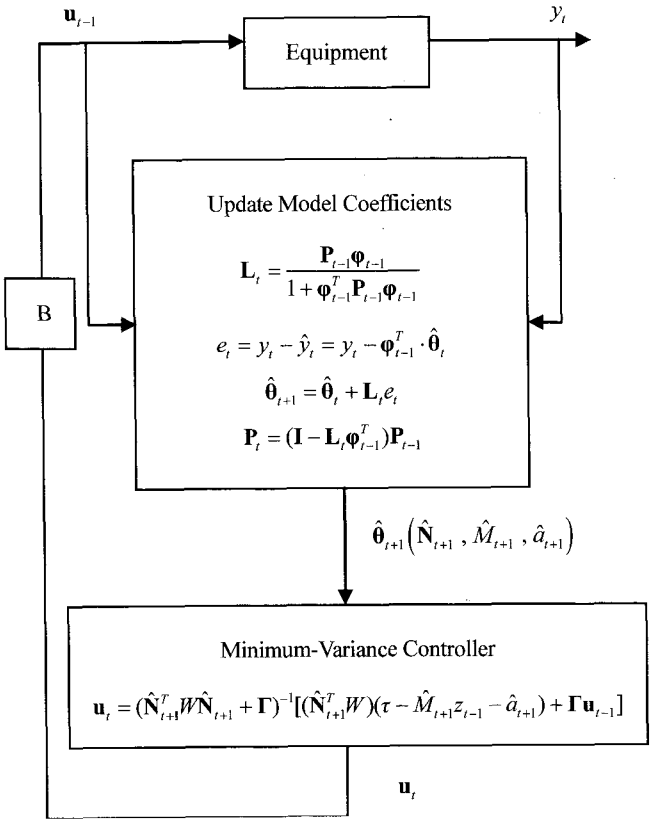

Fig. 3 Block diagram of a DMTMV controller

A RLS algorithm with an exponential discount finds $\hat{\theta}_t$ such that it minimizes

$$\sum_{i=1}^{k} \lambda^{k-i} e_t^2 ,$$

where the one-step-ahead forecast error is defined as

$$e_t = y_t - \hat{y}_t \tag{18}$$

and $\lambda \le 1$ is a factor that discounts old data. We set $\lambda = 1$ for the estimation. The algorithm repeats the following steps for each run t.

1. Compute the gain vector (the weight of the one-step-ahead forecast error) from

$$\mathbf{L}_t = \frac{\mathbf{P}_{t-1}\boldsymbol{\varphi}_{t-1}}{1+\boldsymbol{\varphi}_{t-1}^T\mathbf{P}_{t-1}\boldsymbol{\varphi}_{t-1}} . \tag{19}$$

2. Compute the one-step-ahead forecast error from

$$e_t = y_t - \hat{y}_t = y_t - \boldsymbol{\varphi}_{t-1}^T \cdot \hat{\boldsymbol{\theta}}_t \tag{20}$$

and update the estimate of the coefficient vector

$$\hat{\boldsymbol{\theta}}_{t+1} = \hat{\boldsymbol{\theta}}_t + \mathbf{L}_t e_t . \tag{21}$$

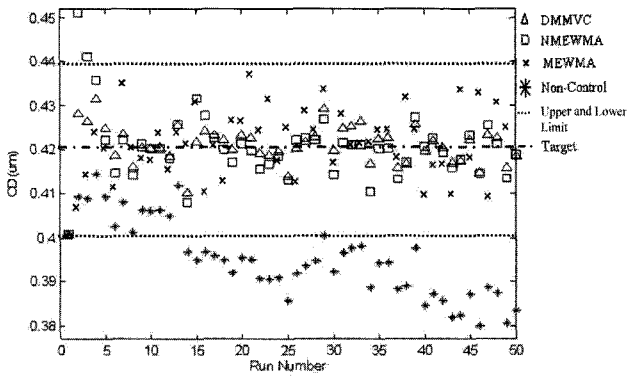

Fig. 4 Process response of the simulations for a 1% disturbance

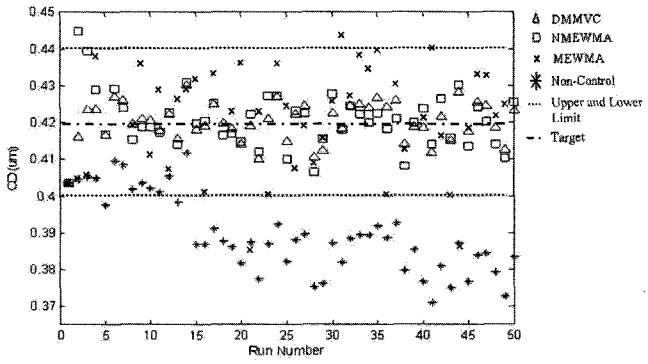

Fig. 5 Process response of the simulations for a 3% disturbance

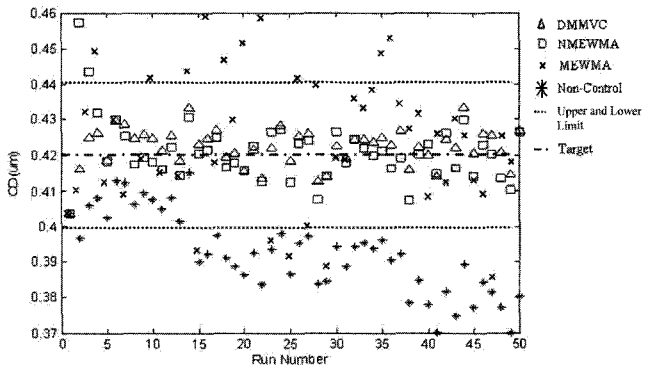

Fig. 6 Process response of the simulations for a 5% disturbance

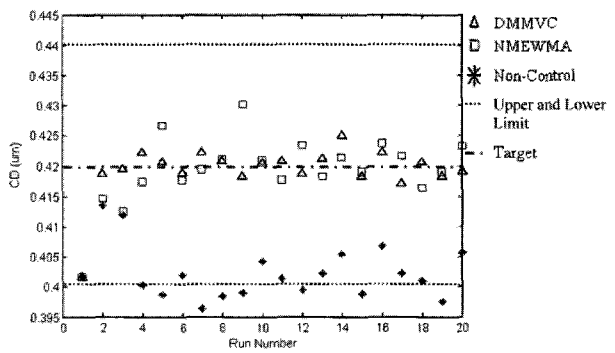

Fig. 7 Process response of the experiments

3. Compute the precision matrix (proportional to the covariance matrix of the coefficient estimates):

$$\mathbf{P}_t = (\mathbf{I} - \mathbf{L}_t \boldsymbol{\varphi}_{t-1}^T)\mathbf{P}_{t-1}. \tag{22}$$

Once the new model coefficients $\hat{\boldsymbol{\theta}}_{t+1}$ are updated, the next run's output $\hat{y}_{t+1}$ can be forecasted from

$$\hat{y}_{t+1} = \boldsymbol{\varphi}_t^T \cdot \hat{\boldsymbol{\theta}}_{t+1} = \hat{\mathbf{N}}_{t+1}\mathbf{u}_t + \hat{M}_{t+1} z_t + \hat{a}_{t+1}. \tag{23}$$

With the minimum-variance control criterion, the one-step controller performance index is

$$\begin{aligned} J &= (\hat{y}_{t+1} - \tau) W (\hat{y}_{t+1} - \tau) + (\mathbf{u}_t - \mathbf{u}_{t-1})' \boldsymbol{\Gamma} (\mathbf{u}_t - \mathbf{u}_{t-1}) \\ &= \left(\hat{\mathbf{N}}_{t+1}\mathbf{u}_t + \hat{M}_{t+1} z_t + \hat{a}_{t+1} - \tau\right) W \left(\hat{\mathbf{N}}_{t+1}\mathbf{u}_t + \hat{M}_{t+1} z_t + \hat{a}_{t+1} - \tau\right). \\ &\quad + (\mathbf{u}_t - \mathbf{u}_{t-1})^T \boldsymbol{\Gamma} (\mathbf{u}_t - \mathbf{u}_{t-1}) \end{aligned} \tag{24}$$

Similar to NMEWMA, one can replace z_t with z_{t-1} in Eq. (24), differentiate it with respect to $\mathbf{u}_t$, and let it equal to zero:

$$\frac{\partial J}{\partial \mathbf{u}_t} = 0. \tag{25}$$

Then, a suboptimal formula of the next run can be obtained from

$$\mathbf{u}_t = (\hat{\mathbf{N}}_{t+1}^T W \hat{\mathbf{N}}_{t+1} + \boldsymbol{\Gamma})^{-1} [(\hat{\mathbf{N}}_{t+1}^T W)(\tau - \hat{M}_{t+1} z_{t-1} - \hat{a}_{t+1}) + \boldsymbol{\Gamma}\mathbf{u}_{t-1}]. \tag{26}$$

A block diagram of the DMTMV controller is shown in Fig. 3.

5. Simulated and Experimental Results

5.1 Simulation

The mean square deviation (MSD) was adopted as the index of the performance, defined as

$$MSD = \sqrt{\frac{1}{n}\sum_{i=1}^{n}(y_i - \tau)^2}, \tag{27}$$

where y_i is the CD and τ is the CD target. The model described by the design of experiments technique and Eq. 1 was treated as the equipment except that different levels of disturbances were added to the model coefficients. Therefore, the equipment model was

$$\begin{aligned} Y_t &= (-0.014895 + \eta_{t-1,1}) X_{t-1,1} + (0.163589 + \eta_{t-1,2}) X_{t-1,2} \\ &\quad + (0.146964 + \eta_{t-1,3}) X_{t-1,2}^2 + (0.424081 + \varepsilon_t) \end{aligned}, \tag{28}$$

where η_1, η_2, η_3, and ε are the coefficient disturbances. The disturbance level was defined as the ratio of the standard deviation of the disturbance versus the equipment model coefficients. The initial linear control model of the MEWMA controller was obtained from a linear multiple regression analysis, expressed as

$$Y_t = -0.014895 X_{t-1,1} + 0.222375 X_{t-1,2} + 0.424081. \tag{29}$$

The initial control models of the DMTMV and NMEWMA controllers with certain model mismatches were set as

$$Y_t = -0.02X_{t-1,1} + 0.2X_{t-1,2} + 0.28X_{t-1,2}^2 + 0.354 . \quad (30)$$

The target of the CD was 0.42 μm and the initial inputs were 2.050 KJ/m^2 for the dose and 0.07 μm for the focus. Three disturbance levels, 1%, 3%, and 5%, were added to the coefficients of the equipment model and 50 runs were simulated. The simulation results are shown in Figs. 4–6. The MSDs of the CDs for the DMTMV, NMEWMA, and MEWMA controllers and a case without any control are listed in Table 2. The simulation results indicate that the DMTMV controller performed better than the NMEWMA and MEWMA controllers.

5.2 Experimental Results

Since the CD and dose can be approximately related to each other by a linear function (see Eq. 2), the conventional run-to-run control of the CD in real photolithography was performed only by adjusting the exposure dose. The linear MISO model was not appropriate for the real lithography process, as verified by the simulation results. Therefore, only the DMTMV and NMEWMA controllers and a case without any control were applied to the real photolithography process to compare their abilities. The CD target and initial inputs were the same as for the simulations. Equation (1), which is built by the design of experiments technique and the multiple regression analysis, was adopted as the initial control model of the DMTMV and NMEWMA controllers. Twenty runs for the DMTMV and NMEWMA controllers and the case without any control were performed in the photolithography area of a clean room. All photolithography and measurement equipment were the same as those used for the experimental design.

Table 2 Mean square derivations of the simulation results

Control Method	1% disturbance	3% disturbance	5% disturbance
DMTMV	0.00531	0.00581	0.00615
NMEWMA	0.00692	0.00836	0.00875
MEWMA	0.00753	0.01961	0.02187
Non-Control	0.02630	0.02960	0.03104

Table 3 Mean square derivations of the experimental results

Control Method	MSD
DMTMV	0.0045
NMEWMA	0.0057
Non-Control	0.0182

The experimental results are shown in Fig. 7. The results indicate that the CD controlled by the DMTMV controller was close to the target from Run 3, and that controlled by the NMEWMA controller was close to the target from Run 6. One can conclude that the DMTMV controller converged better than the NMEWMA controller. The MSDs of the CDs for the two controllers and the case without any control are listed in Table 3. The experimental results indicate that the DMTMV controller performed better overall than the NMEWMA controller.

6. Conclusions

We proposed two valid controllers and applied them to simulated and real photolithography processes. Both controllers possessed the abilities to automatically regulate the model coefficients and could be applied to nonlinear models to reject disturbances and increase yields. Simulated and experimental MSD values of the CDs revealed that the performance of the DMTMV controller was superior to that of the NMEWMA controller.

ACKNOWLEDGMENT

We thank the National Science Council of the Republic of China for financially supporting this study under contract no. NSC 95-2218-E-009-001.

REFERENCES

1. Crisalle, O. D., Soper, R. A., Mellichamp, D. A. and Seborg, D. E., "Adaptive Control of Photolithography," Proceedings of the SPIE, Vol. 1464, pp. 508-526, 1991.
2. Lachman-Shalem, S., Grosman, B. and Lewin, D. R., "Nonlinear Modeling and Multivariate Control of Photolithography," IEEE Transactions on Semiconductor Manufacturing, Vol. 15, No. 3, pp. 310–322, 2002.
3. Grosman, B., Lachman-Shalem, S., Swissa, R. and Lewin, D. R., "Yield Enhancement in Photolithography through Model-based Process Control: Average Mode Control," IEEE Transactions on Semiconductor Manufacturing, Vol. 18, No. 1, pp. 86–93, 2005.
4. Chemali, C. E., Freudenberg, J., Hankinson, M. and Bendik, J. J., "Run-to-Run Critical Dimension and Sidewall Angle Lithography Control Using the PROLITH Simulator," IEEE Transactions on Semiconductor Manufacturing, Vol. 17, No. 3, pp. 388–401, 2004.
5. Yang, D. S., Jung, M. H., Lee, Y. M., Koh, C. W., Yeo, G. S., Woo, S. G., Cho, H. K. and Moon, J. T., "Statistical Analysis of CD SEM Measurement and Process Control in the Indistinguishable Multi-Process Patterns," Proceedings of the SPIE, Vol. 6152, pp. 880-886, 2006.
6. Levinson, H. J., "Principles of Lithography," SPIE Press, pp. 217-225, 2001.
7. Park, S. J., Lee, M. S., Shin, S. Y., Cho, K. H., Lim, J. T., Cho, B. S., Jei, Y. H., Kim, M. K. and Park, C. H., "Run-to-Run Overlay Control of Steppers in Semiconductor Manufacturing Systems Based on History Data Analysis and Neural Network Modeling," IEEE Transactions on Semiconductor Manufacturing, Vol. 18, No. 4, pp. 605–612, 2005.
8. Lee, T. Y., Lee, B. H., Chin, S. B., Cho, Y. S., Hong, J. S., Hong, J. S. and Chang L. S., "Study of Critical Dimension and Overlay Measurement Methodology Using SEM Image Analysis for Process Control," Proceedings of the SPIE, Vol. 6152, pp. 837-844, 2006.
9. Tseng, S. T., Chou, R. J. and Lee, S. P., "A Study on a Multiple EWMA Controller," IIE Transactions, Vol. 34, No. 4, pp.541–549, 2002.
10. Lee, A. C., "Minimum-Variance Controller for a Class of Non-linear Systems," International Journal of Systems Science, Vol. 21, No. 11, pp. 2091–2101, 1990.
11. Castillo, D. E. and Yeh, J. Y., "An Adaptive Run-to-Run Optimizing Controller for Linear and Nonlinear Semiconductor Processes," IEEE Transactions on Semiconductor Manufacturing, Vol. 11, No. 2, pp. 285–295, 1998.
12. Clarke, D. W. and Gawthrop, P. J., "Self-Tuning Controller," Proceedings of the IEE, Vol. 122, No. 9, pp. 929–939, 1975.
13. Belegundu, A. D. and Chandrupatla, T. R., "Optimization Concepts and Application in Engineering," Prentice-Hall, pp. 276-279, 1999.
14. Young, P., "Recursive Estimation and Time-Series Analysis," Springer-Verlag, pp. 42–54, 1984.

15. Liung, L. and Soderstrom, T., "Theory and Practice of Recursive Identification," MIT Press, pp. 16–32, 1986.

16. Graupe, D., "Time Series Analysis, Identification and Adaptive Filtering," Kreger, pp. 63–88, 1989.